CO₂ flux from the volcanic lake of El Chichón (Mexico)

A. Mazot[*] and Y. Taran

Instituto de Geofísica, Universidad Nacional Autónoma de México, Mexico City, Mexico

Resumen

El flujo de dióxido de carbono fue medido en marzo de 2007 en la superficie del lago del Volcán El Chichón, México, usando el método de la cámara de acumulación flotante. Los resultados de 162 medidas y la aplicación del método estadístico estándar, desarrollado para estos estudios, demuestran que la tasa de emisión total de CO_2 del lago cratérico es relativamente alta. La tasa de emisión total calculada con simulación secuencial Gaussiana fue de 164 ± 9.5 t.d^{-1} para el área de superficie del lago de 138, 000 m^2.

Se proponen dos mecanismos diferentes de desgasificación (por difusión a través de la interfase agua-aire y por burbujas) después de usar el método estadístico gráfico (GSA). Los flujos más altos fueron observados a lo largo de trazas de fallas deducidas. Una desgasificación alta también fue observada a lo largo de lineamentos que concuerdan con fallas que afectan el basamento de la región. Si se considera que el flujo promedio de CO_2 comprendiera todo el fondo del cráter (308,000 m^2) se tendría una emisión total del cráter del Volcán El Chichón de por lo menos 370 t.d^{-1}. Este flujo sería cinco veces más alto que el del lago volcánico de Kelud, Indonesia y similar al flujo de CO_2 de otros volcanes activos con desgasificación pasiva en el mundo.

Palabras clave: Flujo de CO_2, cámara de acumulación, lagos cratéricos, El Chichón.

Abstract

Carbon dioxide flux was measured in March 2007 at the surface of the volcanic lake of El Chichón volcano, Mexico using the floating accumulation chamber method. The results of 162 measurements and the application of a standard statistical approach developed for these studies showed that the total CO_2 flux from the crater lake is relatively high. The total emission rate calculated by sequential Gaussian simulation was 164 ± 9.5 t.d^{-1} from the 138,000 m^2 area of the lake. Two different mechanisms of degassing (diffusion through the water-air interface and bubbling) are well resolved by a graphical statistical approach (GSA). The highest fluxes were observed along inferred fault traces. Elevated degassing was also observed along main basement faults in the area. The average flux of CO_2 over the entire crater floor of El Chichón ($\sim$ 308,000 m^2) is inferred to exceed 370 t.d^{-1}. Thus the total emission rate of CO_2 from El Chichón crater is five times higher than at Kelud volcanic lake, Indonesia, but is similar to emission rates from other passively degassing active volcanoes worldwide.

Key words: CO_2 flux, accumulation chamber, crater lakes, El Chichón.

Introduction

Geochemical monitoring of active volcanoes generally includes a periodical or continuous study of the chemistry and/or fluxes of fluids released from the volcano crater or from the volcano edifice where active hydrothermal manifestations are present. In addition to spectroscopic remote sensing of volcanic plumes and direct sampling of fumaroles and hot springs, measurements of the soil diffuse CO_2 degassing by using the method of "accumulation chamber" has become a standard monitoring tool in volcanic and geothermal environments over the last 20 years (e.g. Chiodini *et al.*, 1998). Temporal variations in CO_2 fluxes can be related to changes in the volcanic activity and may be important for the mitigation of the volcanic risk (Hernández *et al.*, 2001a, Notsu *et al.*, 2005). Fluxes of volcanic CO_2 by diffuse degassing through crater floors (Koepenick *et al.*, 1996) or volcanic flanks can be comparable with plume degassing (Wardell *et al.*, 2001). Volcanic craters occupied by a lake include Ruapehu in New Zealand, Poas in Costa Rica, Santa Ana in El Salvador, Kelud in Indonesia and El Chichón in Mexico. In order to measure the gas flux from crater lakes it is necessary to measure fluxes at the water lake surface. Degassing through the lake surface occurs by bubbles (convective/advective degassing) or by diffusion through the water/air interface. Early measurements of diffuse degassing from lakes by using the "floating accumulation chamber" method were made by Kling *et al.* (1991) for studying biogenic CO_2 production from an Arctic lake. Bernard *et al.* (2004) and Mazot (2005) were the first to use this method in a volcanic lake (Santa Ana in El Salvador and Kelud in Indonesia).

In this work, we report the first data on CO_2 flux from the surface of the crater lake of El Chichón volcano, Mexico, obtained in March 2007. The aims of this work were (1) to quantify the total CO_2 output from the volcanic lake and the whole crater, (2) to discriminate between mechanisms of degassing (diffusive or by bubbling); (3) to build a CO_2 flux map of degassing patterns from the lake bottom and relate them to local tectonics.

Finally, the total emission rate of CO_2 from El Chichón volcano is compared with those from other volcanic sites.

General setting

The El Chichón dome complex (17.36N, 93.23W; 1,100 m.a.s.l.) is located in the northwestern part of the State of Chiapas in southeastern Mexico and halfway between the southeastern end of the Trans-Mexican Volcanic Belt (TMVB) and the northwestern end of the Central American Volcanic Arc (CAVA) (Fig. 1A). Prior to the 1982 eruption, the volcanic structure consisted of two nested andesitic lava domes (maximum elevation of 1260 m a.s.l.) inside a somma crater (Macías *et al*, 2003; Layer *et al*., this issue). The 1982 eruption of El
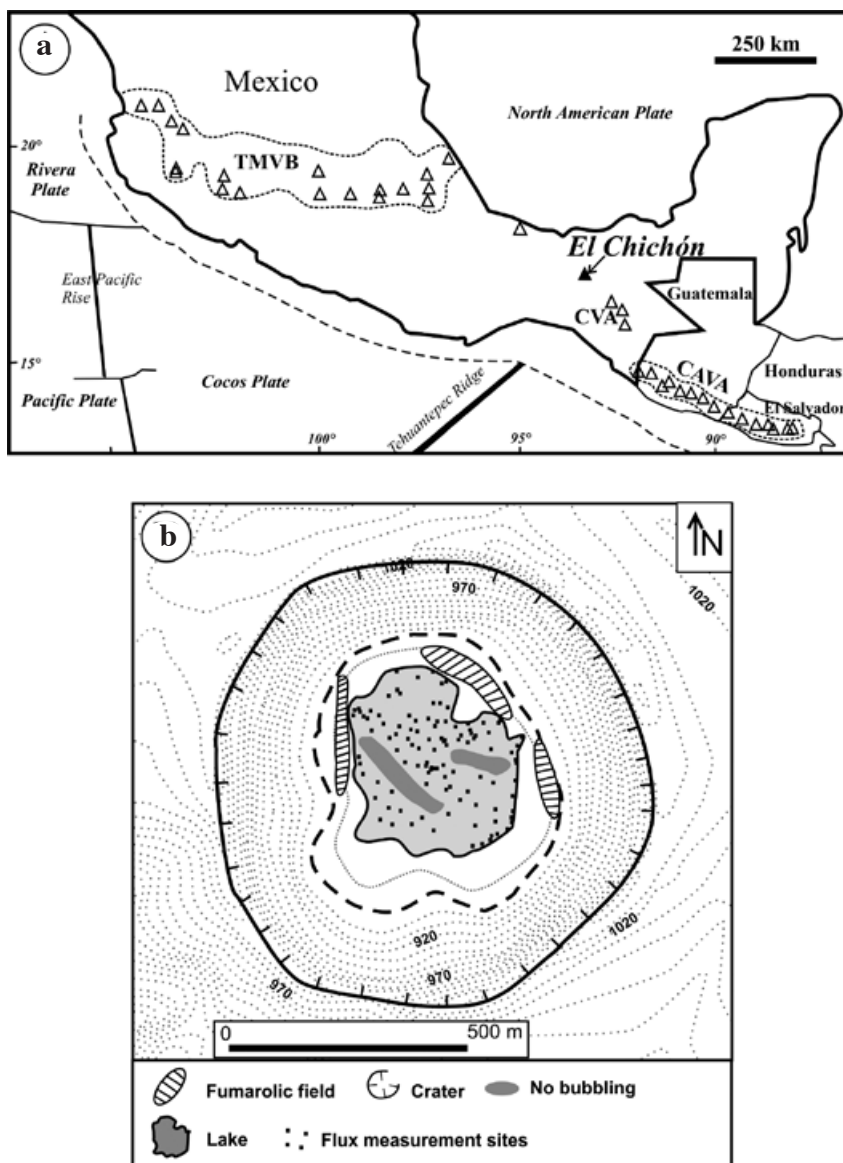

Fig. 1a) Location map of El Chichón volcano in southern Mexico. Modified from Capaccioni et al. (2004). Abbreviations are: TMVB= Trans-Mexican Volcanic Belt, CAVA= Central American Volcanic Arc, CVA= Chiapanecan Volcanic Arc.
b) A sketch map of El Chichón crater with the lake (in gray) as it was in March 2007. The points of measurement are also shown by dots (modified from N. Varley - pers. comm.) Contour interval = 10 m. The 900 m level was chosen for the estimation of the crater floor area (bold-dashed line).

Chichón volcano ejected 1.1 km³ of anhydrite-bearing trachyandesite pyroclastic material to form a new 1-km-wide and 200-m-deep crater (Rose *et al*., 1984). Currently, intense hydrothermal activity, consisting of fumaroles (mainly at the boiling point), steaming grounds, a soap-pool and an acidic (pH≈2.3) and warm lake (~30 °C) occur in the summit crater (Fig. 1B; Taran *et al*., 1998). With the low pH of the lake, CO_2 is mainly present as a gaseous phase and dissolved in water. So, at this range of pH, the other carbonate species HCO_3^- and CO_3^{2-} are not present in the water for which we were sure to measure the whole CO_2 emitted from the lake.

El Chichón lies within an area of folded Jurassic evaporates, Cretaceous limestones, and Tertiary terrigenous rocks (Canul and Rocha, 1981; Duffield *et al*., 1984). The region is affected by two faults systems oriented approximately N-S and E-W. The most significant fault of the latter system is the San Juan Fault (Fig. 2). Furthermore, the area is characterized by a series of N45° E faults (Chapultenango Fault System) on top of which El Chichón has been emplaced (García-Palomo *et al*., 2004).

Procedure and method

In March 2007, a total of 162 randomly distributed CO_2 flux measurements, covering an area of 138,000 m² of the lake surface, were carried out (Fig. 1B). The GPS position of each measurement point represents the average of two readings (resolution ± 6 m) taken before and after each CO_2 flux measurement (duration 40-60 sec). The drift between these two readings depended greatly on the wind and could attain 40 m. The accumulation chamber method (Chiodini *et al*., 1998) was modified in order to work on a lake by using a floating chamber (Fig. 3). Gas flux was measured by using a chamber equipped with a LICOR LI-8100-103 infrared CO_2 analyzer (IRGA). The measurement accuracy of the CO_2 flux measurements method is assumed to be ~12.5% (Evans *et al*., 2001). As the original method from Chiodini *et al*. (1998), the CO_2 gas coming from the water lake passes through the chamber and the infra-red sensor, it returns to the chamber where it accumulates with the new CO_2 entering the chamber. The flux is derived by obtaining the increase of the CO_2 concentration with time (ppmvol.s⁻¹). Each measurement takes about 40 to 60 seconds. In order to
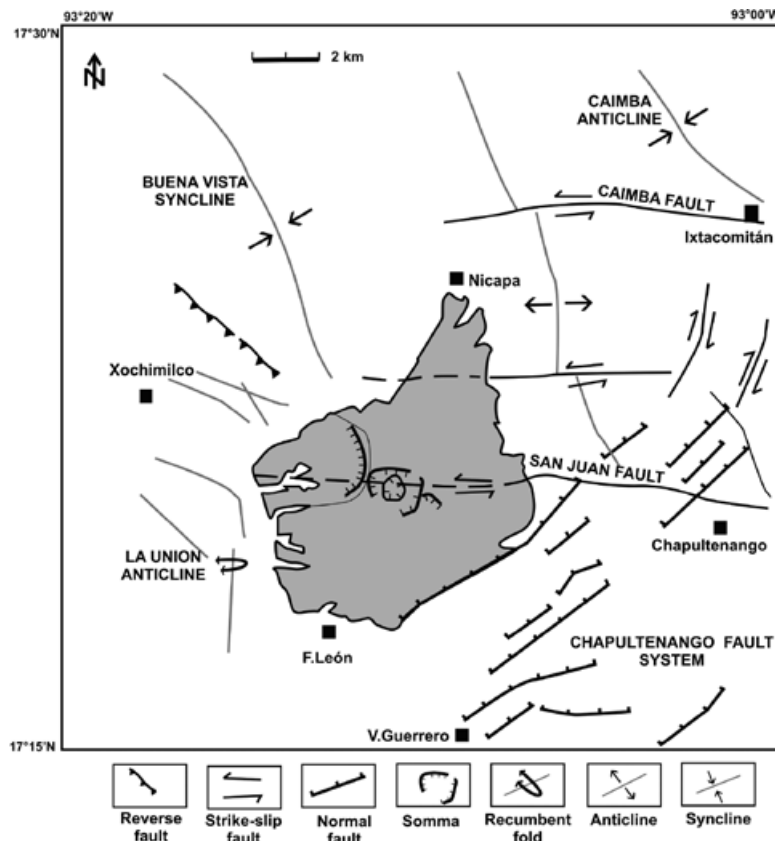

Fig. 2. Structural map of the El Chichón volcano showing main structural features. Modified from Garcia-Palomo *et al*. (2004).

convert volumetric concentrations to mass concentrations ($g.m^{-2}.d^{-1}$), atmospheric pressure, temperature and total volume (sum of the chamber, IRGA connection tube, and the floating device) were taken in account. The fieldwork was undertaken under dry and stable meteorological conditions.

Fig. 3. Picture showing the modifications applied to the accumulation chamber.

Computation of total CO_2 flux was based on the graphical statistical approach (GSA) procedure (Chiodini *et al.*, 1998, 2001; Cardellini *et al.*, 2003). This procedure also permits to differentiate the degassing mechanisms of CO_2. GSA consists in the partition of CO_2 flux data into different lognormal populations (using the so-called "inflection" points) and in the estimation of the proportion, the mean and the standard deviation of each population following the graphical procedure of Sinclair (1974). The CO_2 output associated to each population is obtained by multiplying the area of the lake by the proportion and the mean CO_2 flux. The total CO_2 release from the entire studied area can be obtained by summing the contribution of each population. The 90% confidence interval of the mean is used to calculate the uncertainty of the total CO_2 output estimation of each population.

The mapping of degassing areas and estimation of the total CO_2 discharge from the lake and the uncertainty of this estimation, were performed by using the sequential Gaussian simulation (sGs) that is an interpolation algorithm (Deutsch and Journel, 1998). The basic idea of the sGs is to generate a set of equiprobable representations of the spatial distribution of the simulated values, reproducing the statistical (histogram) and spatial (variogram) characteristics of the original data. According to Goovaerts (2001), the differences among all simulated maps (from 100 to 500 realizations) are used to compute the uncertainty of the flux estimation. The sGs approach has already successfully been used for soil CO_2 degassing at other volcanic systems e.g. Chiodini *et al.*, 2007 and details about the method in Cardellini *et al.*, 2003.

Results and discussion

Probability distribution of the CO_2 flux data

Fig. 4a shows the histogram of log F_{CO2} (where F_{CO2} is CO_2 flux in $g.m^{-2}.d^{-1}$) versus its frequency. The distribution of CO_2 flux differs from a log-normal distribution indicating that there are at least two different mechanisms of degassing through the lake surface. According to the GSA approach (Sinclair, 1974), the histogram must be transferred to a log probability plot (Fig. 4b). This plot indicates that the CO_2 flux data are separated into two different populations recognizable by the inflection point on the curve corresponding to the 83 cumulative percentile. On the plot we can individuate a high CO_2 population (A in fig. 4b) corresponding to the 17 % of the data and a low CO_2 population (B in fig. 4b) corresponding to the 83 % of F_{CO2}. The two-population percentages must be checked and validated by combining both populations in the proportion of 17% A and 83 % B at various levels of log F_{CO2}. The checking procedure uses the following relationship: $P_M = f_A P_A + f_B P_B$, where P_M is the probability of the "mixture", P_A and P_B are cumulative probabilities of population A and B from the plot of Fig. 4b at a specified x value; f_A and f_B are the proportions of populations A and B. In fig. 4b, the points of the "mixture" are represented by gray triangles. Afterwards, parameters of the individual partitioned populations can be estimated. To estimate the arithmetic mean value of CO_2 flux and the central 90% confidence interval of the mean in the original data units (in $g.m^{-2}.d^{-1}$) for each population, we used, according to Chiodini *et al.* (1998), the Sichel's t estimator (David, 1977).

A summary of the estimated parameters of partitioned distributions (populations A and B) is reported in Table 1. Population A is characterized by a mean of 6,702 $g.m^{-2}.d^{-1}$ with a 90% confidence interval of 5,154-10,429 $g.m^{-2}.d^{-1}$. Population B is characterized by a mean of 464 $g.m^{-2}.d^{-1}$

with a 90% confidence interval of 442-490 $g.m^{-2}.d^{-1}$. We suggest that population A corresponds to the flux resulting from bubbles rising through the lake and population B represents the CO_2 degassing by diffusion through the water-air interface (see paragraph 4.3 for details).

The total flow rate of CO_2 released by the lake, calculated by the GSA method, is $(6,702 \ g.m^{-2}.d^{-1} \times 0.17\% + 464 \ g.m^{-2}.d^{-1} \times 0.83\%) \times 138,000 \ m^2 = 210 \ t.d^{-1}$ with a 90% confidence interval of 172-301 $t.d^{-1}$.

Mapping and sgs estimation of the CO_2 flux from the lake

Another statistical method for the estimation of the CO_2 fluxes and the total flow rate is the sequential Gaussian simulation (sGs) (Deutsch and Journel, 1998) method. The 162 measured CO_2 fluxes in randomly distributed points on the lake surface were interpolated by a distribution over a grid of 5,523 square cells (5x5 m^2) covering an area of 138,075 m^2 using the so-called exponential variogram model. Then, 100 simulations

Table 1

Proportions of each population with a mean CO_2 flux (in $g.m^{-2}.d^{-1}$) and a total CO_2 output (in $t.d^{-1}$) obtained by statistical graphical approach.

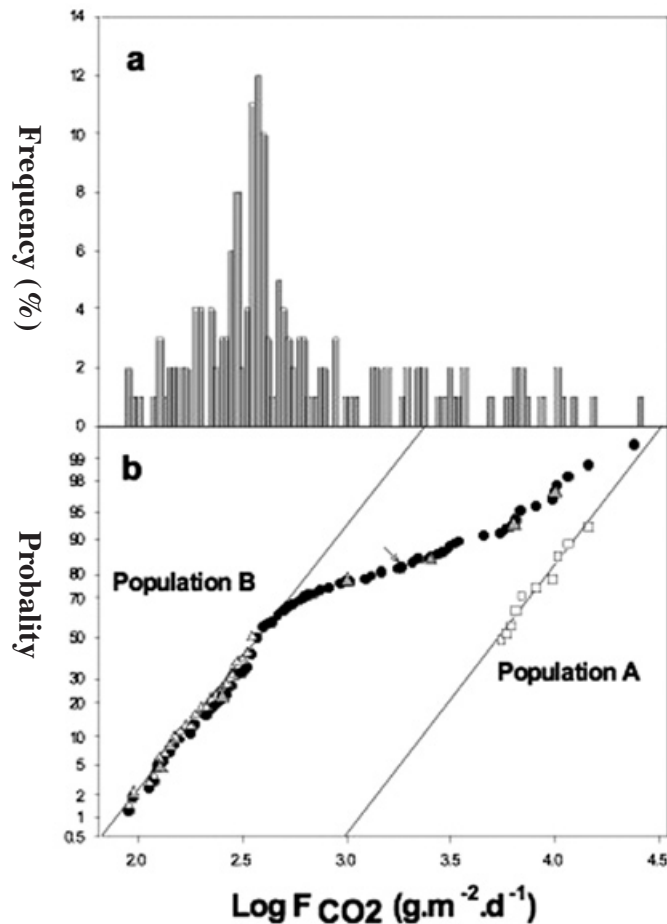| Population of CO_2 flux	Mean flux of CO_2 ($g.m^{-2}.d^{-1}$)	90 % confidence interval ($g.m^{-2}.d^{-1}$)	Proportion (%)	Total CO_2 output for each population ($t.d^{-1}$)	90 % confidence interval ($t.d^{-1}$)	Total CO_2 output ($t.d^{-1}$)
A	6702	5,154-10,429	17	921	708-1433	
B	464	442-490	83	64	61-67	210

Fig. 4. Histogram (a) and probability plot (b) of CO_2 flux data. Population A is indicated by open squares, population B by open triangles and the "mixture" by gray triangles. The inflection point is indicated by an arrow.

of the CO_2 fluxes with the obtained distribution were performed. For each simulation, the CO_2 flux estimated at each cell is multiplied by 25 m^2 and added to the other CO_2 fluxes estimated at the neighborhood cells of the grid to obtain a total lake CO_2 output. The mean of the 100 total simulated CO_2 outputs, 164 t.d^{-1}, represents the estimation of the total CO_2 output from the lake area with a standard deviation of 9.5 t.d^{-1}. The total CO_2 output determined using GSA method is higher (210 t.d^{-1}) than the mean simulated by the sGs method (164 t.d^{-1}). In the calculation of the mean of F_{CO2}, GSA approach does not take into account the spatial correlation between the data, resulting generally in an overestimation of the uncertainty.

The obtained map (Fig. 5) shows that the highest CO_2 flux "spots" are located close to the eastern shore of the lake near the active fumarolic area. Two linear zones of high flux can be clearly recognized on the map, together with several intensively bubbling "funnels" observed during the campaign. These arrangements along NNW-SSE and W-E alignments may be correlated to the regional faults and the E-W San Juan Fault, respectively (García-Palomo *et al*., 2004).

Estimation of the CO_2 diffusion through the lake-air interface

Our suggestion that the population of data with lower

CO_2 fluxes is provided by the diffusion of CO_2 through water-air interface can be checked using the thin boundary layer model (Liss and Slater, 1974). The flux F between water and air may be calculated by the empirical equation (e.g. McGillis and Wanninkhof, 2006):

$$F \ (mg.cm^{-2}.h^{-1}) = k_{CO2} \times (C_{w/a} - C_w) \qquad (1)$$

where k_{CO2} is the gas exchange coefficient (in cm.h^{-1}) for CO_2, C_w and $C_{w/a}$ refers to the concentration of CO_2 in water, and in water film at the water-air interface, respectively.

The value of k_{CO2} was calculated by using the relationship between windspeed and k_{CO2} derived from tracer techniques studies on a small lake (Crusius and Wanninkhof, 2003):

$$k_{CO2} = 0.93 \times u_1 \times [600/Sc_{CO2}]^{-2/3} \qquad (2)$$

where u_1 is the windspeed measured at 1 m height and Sc is defined as the kinematic viscosity of water at measured temperature divided by the diffusivity of the gas at that temperature. Transfer velocity was adjusted to a Schmidt number of 600 that corresponds to the value for the dissolved atmospheric CO_2 in fresh water at 20°C. The value of Sc_{CO2} at 30°C was calculated according to Wanninkhof (1992):
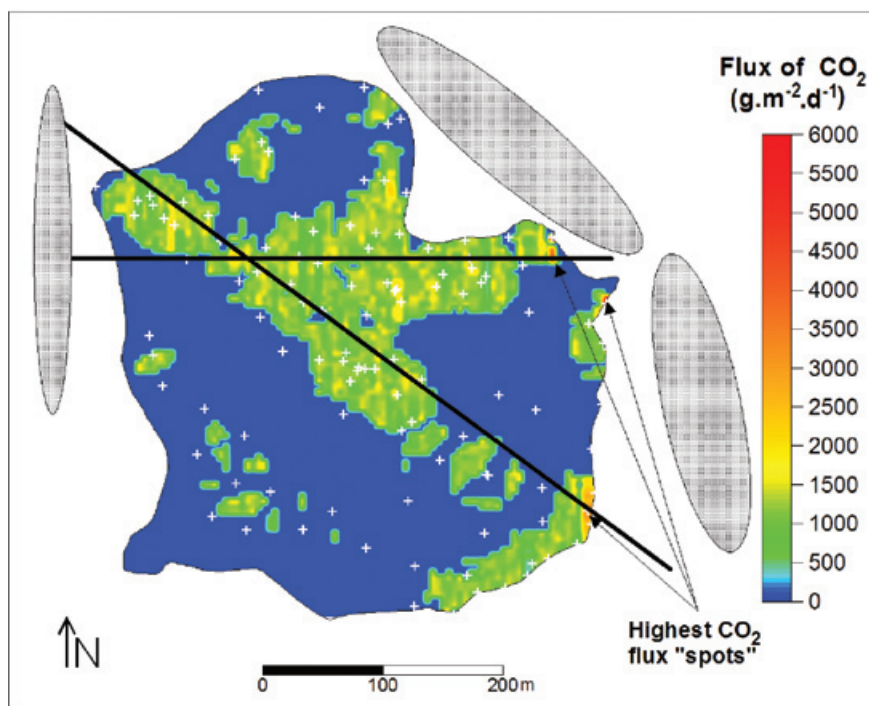

Fig. 5. CO_2 flux map (in g.m^{-2}.d^{-1}) as a mean of 100 sequential Gaussian simulations (see text for explanation). Gray zones indicate fumarolic areas and very high CO_2 fluxes are highlighted. White crosses correspond to the flux measurement sites.

$Sc_{CO2} = 1911.1 - 118.11 \times t + 3.4527 \times t^2 - 0.04132 \times t^3$ (3)

At a mean windspeed u1 of 2 m.s^{-1}, $Sc_{CO2} = 360$ and $k_{CO2} = 1.39$.

At saturation conditions of 30 ºC and 1 atmosphere, C_w of the CO_2 gas is 1.32 mg.cm^{-3} (Eq. 1). The concentration of CO_2 in the air-water ($C_{w/a}$) interface can be approximated to the concentration of CO_2 in the air-saturated water and corresponds to $C_{w/a} \approx 10^{-5}$ mg.cm^{-3} and $C_w \gg C_{w/a}$. From the equation (1) and with values for k_{CO2} of 1.39 and C_w of 1.32 mg.cm^{-3} we estimated a CO_2 flux by diffusion of 442 g.m^{-2}.d-1 that is very close to the mean value of F_{CO2} (464 gm^{-2}d^{-1}) for the low flux of data points (population B).

Estimation of the heat power and comparison with other volcanoes in the world

The area of the whole crater floor corresponding to the isohypse 900 m (Fig. 1b) was estimated to be as 308,000 m^2. Hypothesizing that mains NNW-SSE and W-E alignments are recognized on the lake and that there are not so important variations in F_{CO2} in soil and water due to the low depth of the lake (average depth 3 meters see Taran and Rouwet, 2008), a rough estimate of the total CO_2 output for the whole crater floor yields ~370 t.d^{-1}.

The high CO_2 fluxes plotted on figure 6, show that high CO_2 degassing is not necessarily related to active volcanoes. Three different sources of CO_2 degassing are likely: (1) CO_2, directly coming from a magma chamber, escapes to the surface with other magmatic gases such as SO_2, H_2S, HCl and HF, as this is the case for volcanoes Masaya, Nicaragua (Pérez *et al.*, 2000), Miyakejima and Usu, Japan (Hernández *et al.*, 2001a,b), Stromboli, Italy (Carapezza and Federico, 2000), San Salvador, El Salvador (Pérez *et al.*, 2004), Santa Ana, El Salvador (Bernard *et al.*, 2004) and Galeras, Colombia (Williams-Jones *et al.*, 2000). (2) CO_2 coming from a magma chamber but with a possible contamination due to the crustal carbonate decomposition and subsequent CO_2 release. This type of the CO_2 release could be the case for Solfatara and Vesuvio, Italy (Cardellini *et al.*, 2003; Frondini *et al.*, 2004), Santorini and Nisyros, Greece (Chiodini *et al.*, 1998; Cardellini *et al.*, 2003), Yellowstone, USA (Werner *et al.*, 2000) and Kelud, Indonesia (Mazot, 2005). (3) CO_2 degassing at low temperature and coming from carbonate metamorphism, not related to magmatism. Sites that released this kind of CO_2 are for example Dixie Valley, USA (Bergfeld *et al.*, 2001) and central Italy (Rogie *et al.*, 2000).
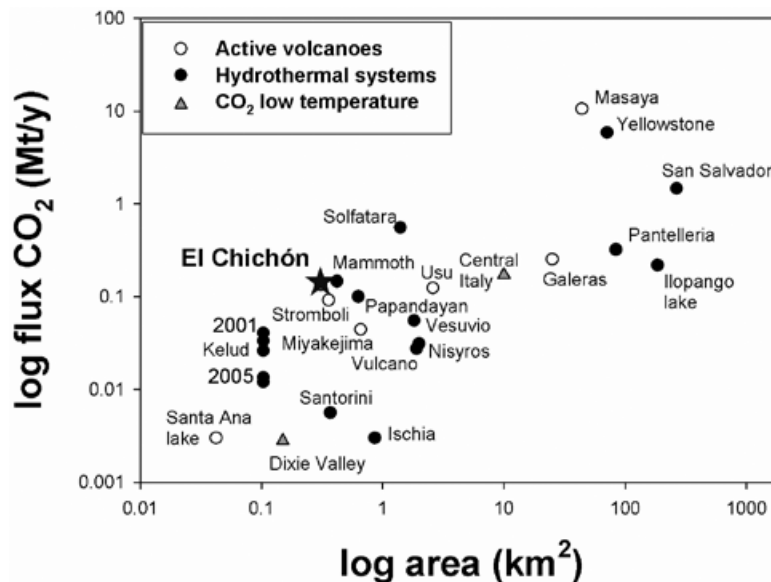

Fig. 6. Comparison of CO_2 flux (in Mt/y) among El Chichón crater lake and other volcanic and geothermal sites in the world: Vulcano (Baubron *et al.*, 1990), Stromboli (Carapezza and Federico, 2000), Solfatara (Cardellini *et al.*, 2003), Ischia (Chiodini *et al.*, 2004), Vesuvio (Frondini *et al.*, 2004), Central Italy (Rogie *et al.*, 2000), Pantelleria, Italy (Favara *et al.*, 2001); Dixie Valley (Bergfeld *et al.*, 2001), Mammoth Mountain (Sorey *et al.*, 1998), Yellowstone, USA (Werner *et al.*, 2000); Santa-Ana (Bernard *et al.*, 2004), San Salvador, (Pérez *et al.*, 2004), Ilopango lake, El Salvador (López *et al.*, 2004); Santorini, (Chiodini *et al.*, 1998), Nisyros, Greece (Cardellini *et al.*, 2003); Usu (Hernández *et al.*, 2001a), Miyakejima, Japan (Hernandez *et al.*, 2001b); Kelud, Indonesia (Mazot, 2005); Masaya, Nicaragua (Pérez *et al.*, 2000); Galeras, Colombia (Williams-Jones, 2000).

The total CO_2 output from El Chichon crater is 1.5 times higher than the effusion rates reported for the summit area at Stromboli (mean flux: 246 t.d^{-1}; area: 357,500 m^2; Carapezza and Federico, 2000) and little lower than those reported for the soil CO_2 flux at Mammoth Mountain in Long Valley Caldera, USA (mean flux: 411 t.d^{-1}; area: 420,000 m^2; Sorey *et al.*, 1998).

The CO_2 degassing from the volcanic lake of El Chichón was compared (Fig. 6) with that of Kelud crater lake (Indonesia) and Santa Ana crater lake (El Salvador). In the Kelud crater lake, where CO_2 flux measurements has been carried out since 2001 (Mazot, 2005), the total CO_2 output ranges from 100 t.d^{-1} with a mean of 1020 g.m^{-2}.d^{-1} (2001) to 35 t.d^{-1} with a mean of 335 g.m^{-2}.d^{-1} (2006) and a constant area of 103,600 m^2. In Santa Ana, where measurement was performed in 2002, CO_2 output corresponds to 7 t.d^{-1} in 2002 with a mean of CO_2 flux of 220 g.m-2.d^{-1} and an area of 30,000 m^2 (Bernard *et al*, 2004). Among these three volcanic lakes, the total CO_2 output at El Chichón in 2007 was up to 5 times higher (164 t.d^{-1}) than Kelud volcano and 23 times higher than Santa Ana (Fig.4).

Fumarolic gas of El Chichón volcano contains about 90 wt% of H_2O (steam) and 10 wt% of CO_2 (Taran *et al.*, 1998; Tassi *et al.*, 2003). Assuming that all the CO_2 released from the crater floor is the result of separation of these gases caused by shallow condensation of hydrothermal steam at ~ 100 °C, beneath the crater floor of the volcano we have $\sim 3,700$ t/day or ~ 43 kg/s of steam flux and beneath the lake we have $\sim 1,640$ t/day or ~ 19 kg/s. Using a value for steam enthalpy at 100 °C due to steam condensation (~ 2.257 MJ/kg) we can estimate the heat power due to fumarolic output from the crater floor as 100 and from the lake 43 MW. This heat output is up to 3.5 times higher than the output estimated by Taran and Rouwet (2008) using the heat and chemical balance approach at El Chichón lake. Our estimation based on the direct measurements of fluxes seems to be more realistic.

The heat output corresponding to El Chichón lake (43 MW) is comparable with the heat power of other crater lakes of active volcanoes. In Kelud lake, Mazot (2005) calculated values of heat power ranging from 45 to 180 MW in the period 2004-2007 (Table 2) by using the heat and chemical balance model of Stevenson (1992). The heat power was estimated on other crater lakes as Kawah Ijen (Indonesia; Delmelle, 1995), Taal (Philippines; Poussielgue, 1998), Poas (Costa Rica; Stevenson, 1992), Yugama (Japan; Ohba *et al.*, 1994), Ruapehu (New Zealand; Stevenson, 1992) and Copahue (Argentina; Varekamp *et al.*, 2001). The heat output of 100 MW from El Chichón crater is relatively small in comparison with the heat power observed at hot (>40 °C) crater lakes,

where values as high as several hundred MW were estimated (Table 2).

Table 2

Heat power (in MW) discharged by crater lakes in the world.

	date	E_{IN} (MW)	
Santa Ana	2002	16	Bernard *et al.* (2004)
Yugama	1988-1993	3-22	Ohba (1994)
Copahue	1997-1999	7-45	Varekamp *et al.* (2001)
El Chichón	1997-2007	20-43	This study and Taran and Rouwet (2008)
Kelud	2001-2007	45-180	Mazot (2005)
Taal	1989-1995	200-350	Poussielgue (1998)
Kawah Ijen	1980-1993	271-378	Delmelle (1995)
Poas	1978-1989	100-400	Stevenson (1992)
Ruapehu	1966-1989	50-1000	Stevenson (1992)

Conclusion

CO_2 flux measurements made by using the floating accumulation chamber method allowed to estimate the total CO_2 emission from the crater lake of El Chichón (138,000 m^2) to be close to 164 t.d^{-1}. For the total area of the crater floor of 308,000 m^2 the total CO_2 emission was estimated at 370 t.d^{-1}. This level of the total CO_2 emission and the estimated heat output are comparable with other volcanic and geothermal areas worldwide.

Continuous monitoring of CO_2 flux from the crater lake of El Chichón could improve our understanding of the hydrothermal system. This would be complementary to other geochemical investigations and it would be particularly important for detecting possible changes in the activity of the volcano.

Bibliography

Baubron, J. C., P. Allard, J. C. Sabroux, D. Tedesco and J. P. Toutain, 1990. Soil gas emanations as precursory indicators of volcanic eruptions, *J. Geol. Soc. London, 148*, 571-576.

Bergfeld, D., F. Goff and C. J. Janik, 2001. Elevated carbon dioxide flux at the Dixie Valley geothermal field, Nevada; relations between surface phenomena and the geothermal reservoir. *Chem. Geol., 177,* 43-66.

Bernard, A., C. D. Escobar, A. Mazot and R. E. Gutiérrez, 2004. The acid volcanic lake of Santa Ana volcano, El Salvador. *GSA Special Paper, 375*, 121-134.

Canul, R. F. and V. L. Rocha, 1981. Informe geológico de la zona geotérmica de "El Chichonal," Chiapas: Comisión Federal de Electricidad, Informe (Unpublished internal report).

Capaccioni, B., Y. Taran, F. Tassi, O. Vaselli, F. Mangani and J. L. Macías, 2004. Source conditions and degradation processes of light hydrocarbons in volcanic gases: an example from El Chichón volcano (Chiapas State, Mexico). *Chem. Geol., 206*, 81-96.

Carapezza, M. L and C. Federico, 2000. The contribution of fluid geochemistry to the volcano monitoring of Stromboli. *J. Volcanol. Geotherm. Res., 95*, 227-245.

Cardellini, C., G. Chiodini and F. Frondini, 2003. Application of stochastic simulation to CO_2 flux from soil: mapping and quantification of gas release. *J. Geophys. Res. 108, 2425*, doi:10.1029/2002JB002165.

Chiodini, G., R. Avino, T. Brombach, S. Caliro, C. Cardellini, S. De Vita, F. Frondini, D. Granirei, E. Marotta and G. Ventura, 2004. Fumarolic and diffuse soil degassing west of Mount Epomeo, Ischia, Italy. *J. Volcanol. Geotherm. Res., 133*, 291-309

Chiodini, G., R. Cioni, M. Guidi, B. Raco and L. Marini, 1998. Soil CO_2 flux measurements in volcanic and geothermal areas. *Appl. Geochem., 13, 5*, 543-552.

Chiodini, G., F. Frondini, C. Cardellini, D. Granieri, L. Marini and G. Ventura, 2001. CO_2 degassing and energy release at Solfatara volcano, Campi Flegrei, Italy. *J. Geophys. Res. 106, B8*, 16,213-16,221.

Chiodini, G., A. Baldini, F. Barberi, M. L. Carapezza, C. Cardellini, F. Frondini, D. Granieri, and M. Ranaldi, 2007. Carbon dioxide degassing at Latera caldera (Italy): Evidence of geothermal reservoir and evaluation of its potential energy. *J. Geophys. Res., 112, B12204*, doi:10.1029/2006JB004896.

Crusius, J. and R. Wanninkhof, 2003. Gas transfer velocities measured at low wind speed over a lake. *Limnol. Oceanogr., 48*, 1010-1017.

David, M., 1977. Geostatistical ore reserve estimation (Developments in geomathematics 2). Elsevier, New-York, 363 pp.

Delmelle, P., 1995. Geochemical, isotopic and heat budget study of two volcano hosted hydrothermal systems: the acid crater lakes of Kawah Ijen, Indonesia, and Taal, Philippines, volcanoes. PhD thesis, Université Libre de Bruxelles, Brussels, 247 pp.

Deutsch, C. V. and A. G. Journel, 1998. GSLIB: Geostatistical Software Library and Users Guide, 2nd ed., 369 pp, Oxford Univ. Press, New York.

Duffield, W. A., R. I. Tilling and R. Canul, 1984. Geology of Chichón Volcano, Chiapas, Mexico. *J. Volcanol. Geotherm. Res., 20*, 117–132.

Evans, W. C., M. L. Sorey, B. M. Kennedy, D. A. Stonestrom, J. D. Rogie and D. L. Shuster, 2001. High CO_2 emissions through porous media : transport mechanisms and implications for flux measurement and fractionation. *Chem. Geology, 177*, 15-29.

Favara, R., S. Giammanco, S. Inguaggiato and G. Pecoraino, 2001. Preliminary estimate of CO_2 output from Pantelleria Island volcano (Sicily, Italy): evidence of active mantle degassing. *Appl. Geochem., 16*, 883-894.

Frondini, F., G. Chiodini, S. Caliro, C. Cardellini, D. Granieri and G. Ventura, 2004. Diffuse CO_2 degassing at Vesuvio, Italy. *Bull. Volcanol, 66*, 642–651.

García-Palomo, A., J. L. Macías and J. M. Espíndola, 2004. Strike-slip faults and K-alkaline volcanism at El Chichón volcano, southeastern Mexico. *J. Volcanol. Geotherm. Res., 136*, 247-268.

Goovaerts, P., 2001. Geostatistical modelling of uncertainty in soil science. *Geoderma, 103*, 3-26.

Hernández, P. A., K. Notsu, J. M. Salazar, T. Mori, G. Natale, H. Okada, G. Virgili, Y. Shimoike, M. Sato and N. M. Perez , 2001a. Carbon dioxide degassing by advective flow from Usu Volcano, Japan. *Science, 292*, 83-86.

Hernández, P. A., J. M. Salazar, Y. Shimoike, T. Mori, K. Notsu and N. M. Perez , 2001b. Diffuse emission of CO_2 from Miyakejima volcano, Japan. *Chem. Geol., 177*, 175-185.

Kling, G. W., G. W. Kipphut and M. C. Miller, 1991. Artic Lakes and Streams as Gas Conduits to the Atmosphere: Implications for Tundra Carbon Budgets. *Science, 251*, 298-301.

Koepenick, K. W., S. L. Brantley, J. M. Thompson, G. L. Rowe, A. Nyblade and C. Moshy, 1996. Volatile emissions from the crater and flank of Oldoinyo Lengai volcano, Tanzania. *J. Geophys. Res., 101, B6*, 13819-13830.

Layer, P. W., A. García-Palomo, Jones, J. L. Macías, J. L. Arce and J. C. Mora, 2008. El Chichón Volcanic Complex, Chiapas, Mexico: stages of evolution based on field mapping and $^{40}Ar/^{39}Ar$ geochronology. *Geofís. Int.*, *48-1*, 33-54.

Liss, P. S. and P. G. Slater, 1974. Flux of gases across the air-sea interface. *Nature, 247*, 181-184.

López, D., L. Ransom, N. Pérez, P. Hernández and J. Monterrosa, 2004. Dynamics of diffuse degassing at Ilopango Caldera, El Salvador. *GSA Special Paper, 375,* 191-202.

Macías, J. L., J. L. Arce, J. C. Mora, J. M. Espíndola, R. Saucedo and P. Manetti, 2003. A 550-year-old Plinian eruption at El Chichón Volcano, Chiapas, Mexico: Explosive volcanism linked to reheating of the magma reservoir. *J. Geophys. Res., 108, B12, 2569*, doi:10.1029/2003JB002551.

Mazot, A., 2005. CO_2 degassing and fluid geochemistry at Papandayan and Kelud volcanoes, Java Island, Indonesia. Ph. D. Thesis, Université Libre de Bruxelles, Brussels, 294 pp.

Mcgillis, W. R. and R. Wanninkhof, 2006. Aqueous CO_2 gradients for air–sea flux estimates. *Mar. Chem., 98*, 100-108.

Notsu, K., K. Sugiyama, M. Hosoe, A. Uemura, Y. Shimoike, F. Tsunomori, H. Sumino, J. Yamamoto, T. Mori and P. A. Hernández, 2005. Diffuse CO_2 efflux from Iwojima volcano, Izu-Ogasawara arc, Japan. *J. Volcanol. Geotherm. Res., 139*, 147-161.

Ohba, T., J. I. Hirabayashi and K. Nogami, 1994. Water, heat and chloride budgets of the crater lake, Yugama at Kusatsu-Shirane volcano, Japan. *Geochem. J., 28*, 217-231.

Pérez, N., J. Salazar, P. Hernández, T. Soriano, D. L. López and K. Notsu, 2004. Diffuse degassing of CO_2 from Masaya caldera, Central America. *GSA Special Paper, 375*, 227-236.

Pérez, N., J. Salazar, A. Saballos, J. Álvarez, F. Segura, P. Hernández and K. Notsu, 2000. Diffuse degassing of CO_2 from Masaya caldera, Central America. *Eos Trans AGU, Fall Meet Suppl.*

Poussielgue, N., 1998. Signal acoustique et activité thermique dans les lacs de cratère de volcans actifs. Réalisation d'une station de mesure hydroacoustique au Taal (Philippines). Ph. D. Thesis, Université de Savoie, Chambéry, France, 246 pp.

Rogie, J. D., D. M. Kerrick, G. Chiodini and F. Frondini, 2000. Flux measurements of nonvolcanic CO_2 emission from some vents in central Italy. *J. Geophys. Res., 105, B4*, 8435-8445.

Rose, W. I., T. J. Bornhorst, S. P. Halsor, W. A. Capaul, P. S. Plumley, S. R. De La Cruz, M. Mena and R. Mota, 1984. Volcán El Chichón, Mexico: Pre-1982 S-rich eruptive activity. *J. Volcanol. Geotherm. Res.,23*, 147-167.

Sinclair, A. J., 1974. Selection of threshold values in geochemical data using probability graphs. *J. Geochem. Explor., 3*, 129-149.

Sorey, M. L., W. C. Evans, B. M. Kennedy, C. D. Farrar, L. J. Hainsworth and B. Hausback, 1998. Carbon dioxide and helium emissions from a reservoir of magmatic gas beneath Mammoth Mountain, California. *J. Geophys. Res. 103, B7*, 15303–15323.

Stevenson, D. S., 1992. Heat transfer in active volcanoes: models of crater lake systems. Ph. D. Thesis, The Open University, United Kingdom, 235 pp.

Taran, Y., T. P. Fisher, B. Pokrovsky, Y. Sano, M. Armienta and J. L. Macías, 1998. Geochemistry of the volcano-hydrothermal system of El Chichon Volcano, Chiapas, Mexico. *Bull. Vol., 59*, 436-449.

Taran, Y. and D. Rouwet, 2008. Estimating thermal inflow to El Chichón crater lake using the energy-budget, chemical and isotope balance approaches. *J. Volcanol. Geotherm. Res. 175*, 472-481.

Tassi, F., O. Vaselli, B. Capaccioni, J. L. Macías, A. Nencetti, G. Montegrossi and G. Magro, 2003. Chemical composition of fumarolic gases and spring discharges from El Chichón volcano, Mexico: causes and implications of the changes detected over the period 1998-2000. *J. Volcanol. Geotherm. Res., 123*, 105-121.

Varekamp, J. C., A. P. Ouimette, S. W. Herman, A. Bermudez and D. Delpino, 2001. Hydrothermal element fluxes from Copahue, Argentina: A "beehive" volcano in turmoil. *Geology, 29, 11*, 1059-106.

Wanninkhof, J., 1992. Relationship between wind speed and gas exchange over the ocean. *J. Geophys. Res., 97, C5*, 7373-7382.

Wardell, L. J., P. R. Kyle, N. Dunbar and B. Christenson, 2001. White Island volcano, New Zealand : carbon dioxide and sulfur dioxide emission rates and melt inclusion studies. *Chemical Geology, 177*, 187-200.

Werner, C., S. L. Brantley and K. Boomer, 2000. CO_2 emissions related to the Yellowstone volcanic system 2. Statistical sampling, total degassing, and transport mechanisms. *J. Geophys. Res., 105, B5*, 10,831-10,846.

Williams-Jones, G., J. Stix, M. Heiligmann, A. Charland, B. Sherwood Lollar, N. Arner, G. Garzón V., J. Barquero and E. Fernandez, 2000. A model of diffuse degassing at three subduction-related volcanoes. *Bull Volcanol, 62*, 130-142.

A. Mazot[*] and Y. Taran

Instituto de Geofísica, Universidad Nacional Autónoma de México, Del. Coyoacán, 04510 Mexico City, Mexico

E-mail: taran@geofisica.unam.mx

Corresponding author: amazot@geofisica.unam.mx